Arch. Metall. Mater. **62** (2017), 4, 2455-2460

DOI: 10.1515/amm-2017-0361

P. LEDWIG*#, B. DUBIEL*

MICROSTRUCTURE AND CORROSION RESISTANCE OF COMPOSITE nc-TiO_2/Ni COATING ON 316L STEEL

The aim of this work was to obtain composite of nc-TiO_2/Ni coatings on 316L steel and to characterize their corrosion resistance. In order to investigate the influence of the addition of TiO_2 nanoparticles, both pure Ni and composite nc-TiO_2/Ni coatings were electrodeposited from nickel citrate baths. The microstructure of the coatings was examined by scanning and transmission electron microscopy. The nc-TiO_2/Ni coatings were about 10 μm thick. Their microstructure consisted of TiO_2 nanoparticles uniformly distributed in nanocrystalline Ni matrix. The corrosion resistance of the coatings was measured using impedance spectroscopy and polarization curves techniques in Ringer's solution. It was determined that the addition of nano-TiO_2 particles improved corrosion resistance and reduced corrosion rate of the coated steel.

Keyword: nc-TiO_2/Ni coatings, electrodeposition, nanocomposite, microstructure, corrosion resistance

1. Introduction

Electroplating is one of the most commonly used methods to obtain nickel coatings or composite nickel-base coatings reinforced by nonmetallic particles on the steel surfaces [1-5]. Addition of second phase particles is beneficial due to the enhancing hardness, mechanical properties and corrosion resistance. The electrodeposition process has many advantages like rapid deposition rate, homogeneous distribution of reinforcement particles, and low cost [5,6].

In the present work, our attention was focused on deposition and characterization of nickel martix composite coatings containing TiO_2 nanoparticles. Such coatings are of a great interest in terms of their corrosion resistance as well as photocatalytic properties, which are used in self-cleaning and germicidal surfaces or for removal many impurities [1-6]. Technology of nickel films electrodeposition on steel substrate with use of Watt's bath is well known. Recently researchers suggest to replace the Watt's bath by less toxic one, e.g. citric/sulfate bath, in which boric anions are replaced by citric anions [7,8].

Composites containing nickel and TiO_2 are widely studied mainly because of the great photocatalytic effect of nc-TiO_2 particles. Applications based on TiO_2 matrix doped by nickel were used for utilization of CO_2 [9,10]. Another specific uses for these composites are an electrode to hydrogen production [11], air purification [12], antireflection coatings for solar application [13] or self-cleaning surfaces [14]. Such materials are mostly deposited in the form of coatings in purpose of improvement the substrate properties.

The composite nc-TiO_2/Ni coatings obtained by electrodeposition were already examined by others, e.g. [1-6]. Additionally many modifications of Ni matrix like Ni-Zn [15], Ni-W [16], Ni-B [17], Ni-Co [18], Ni-Mo [19] were investigated. The co-deposition of TiO_2 with graphene nanosheets (GNS) in Ni matrix was also successfully demonstrated [20]. As the substrate material mainly mild steel or cooper were used. Most of the nc-TiO_2/Ni coatings examined previously was deposited using classic Watts baths, e.g. [1,6,18,20]. The citric-sulfate bath, which was used for deposition nc-TiO_2/Ni coatings in this study, is a good alternative to Watts bath. The available results of the research on the electrolytically deposited nc-TiO_2/Ni coatings are mainly focused on the mechanism of co-deposition and determination of current conditions, microstructure, corrosion resistance and mechanical properties of the coatings [1-6].

The aim of this work was to deposit nc-TiO_2/Ni coatings on 316L steel using citric-sulfate bath and characterize their microstructure and corrosion resistance in the Ringer's solution.

2. Materials and methods

Coatings were deposited on the rectangular steel plates of 15 mm ×30 mm ×0.5 mm made of AISI 316L stainless steel with nominal chemical composition: ≤0,03 C, 17,5 Cr, 11,5 Ni, ≤2,0 Mn, 2,3 Mo, ≤0,11 other, balance Fe (wt %). The plates were polished using abrasive sand papers of 2 000 gradation. The plates were washed using distilled water and ethanol in ultrasonic cleaner.

* AGH UNIVERSITY OF SCIENCE AND TECHNOLOGY, FACULTY OF METALS ENGINEERING AND INDUSTRIAL COMPUTER SCIENCE, AL. A. MICKIEWICZA 30, 30-059 KRAKÓW, POLAND

Corresponding author: pledwig@agh.edu.pl

The intermediate undercoat consisting of Ni and Cu layers about 1 μm thick was deposited. The purpose of Cu undercoat was to reduce stress in the Ni-based coating, what allowed the deposition of thicker coatings. The external nc-TiO_2/Ni coatings with concentration of TiO_2 powder from 2 g/L to 10 g/L were deposited using nano-TiO_2 powder (Aldrich, 21 nm particle size).

Chemical composition of the electrolytic baths used as the source of copper and nickel for deposition of the coatings are given in tables 1 and 2, respectively. In case of deposition of composite coatings the bath was enriched by different concentration of TiO_2 nanopowder.

TABLE 1

Composition and parameters of copper electrolytic bath

Compound/Parameter	
$CuSO_4.5H_2O$	200 g/L
H_2SO_4	50 g/L
Current density	2.5 A/dm^2
Temperature	35 °C

TABLE 2

Composition and parameters of TiO_2/Ni electrolytic bath

Compound/parameter	Concentration
$NiSO_4.H_2O$	350 g/L
$NiCl_2{\cdot}H_2O$	85 g/L
Citric acid	30 g/L
NaOH	Until obtaining pH=4
TiO_2	0, 2, 4, 6, 8, 10 g/L
Current density	1 - 2.5 A/dm^2
Temperature	50-55°C
pH	4

Zeta potential (ζ) of electrolytic bath containing TiO_2 particles was measured using ZetaSizer Nano-ZS 90 of Malvern.

Coatings were deposited using potentiostat/galvanostat PGSTAT 302N of Autolab in three electrode mode, where the counter electrode was nickel or copper plate and reference was saturated Ag/AgCl electrode. Current density range from 1 A/dm^2 to 2.5 A/dm^2 was used.

Electrochemical properties of coatings, like electrochemical corrosion resistance and impedance spectroscopy, were measured in the Ringer's solution using three-electrode system with platinum plate as a counter electrode. The polarization curves method was used to determinate corrosion resistance of materials. Based on linear polarization using Tafel extrapolation method the corrosion rate of material was extrapolated. The Nova 2.0 software was applied to determine values of corrosion current, corrosion potential, corrosion rate and parameters of equivalent circuit.

The microstructure of obtained coatings was examined by scanning electron microscope (SEM) FEI Inspect and FEI Nova Nanoscan 450 and transmission electron microscope (TEM) Jeol JEM-2010 ARP equipped with scanning-transmission (STEM) device. Thin foils for TEM examination were prepared by jet electropolishing form the plan-view sections of the nc-TiO_2/Ni coatings. Chemical composition in nanoareas was determined using energy dispersive X-ray spectroscopy (EDS)

Results and discussion

Zeta potential of TiO_2 particles in electrolytic bath

The stability of the TiO_2 particles in electrolytic bath was determined by zeta potential measurement. The nickel electrolytic bath was diluted 10 times and the TiO_2 particles in concentration of 0.1 g/L were added to the bath. Particles were stirred and ultrasonicated for 15 minutes to evenly distribute them in the suspension and minimize the size and amount of TiO_2 agglomerates.

The zeta potential of TiO_2 nanoparticles in diluted bath was equal to –8 ±1.9 mV. Negative value of zeta potential indicated electrophoretic mobility of nanoparticles towards the anode. The low value of zeta potential corresponds to the low stability of nanoparticles in the suspension [21]. It was observed that stability of the suspension was rather poor and the sedimentation of particles was visible after few minutes. The suspensions were completely separated after 30 minutes without stirring. This could be a reason of the lack of electophoretical TiO_2 deposit on the counter electrode surface. To overcome the opposite electrophoretic mobility and create the composite nc-TiO_2/Ni coating it was necessary to apply mechanical stirring of the bath during the deposition using magnetic stirrer.

Microstructure

TiO_2 nanoparticles used for deposition of composite coatings exhibited oval and polyhedral morphology and their equivalent diameter was in the range from 15 nm to 85 nm. Electron diffraction investigation revealed that the nanopowder is the mixture of two TiO_2 phases, namely anatase (tetragonal system, space group I41/a m d) and rutile (tetragonal system, space group P42/m n m).

The microstructure of the coatings highly depended on the parameters of deposition. Lower current density ensured the lower deposition rate. The effect of temperature was noticeable and for the temperature lower than 55°C obtained coatings were thinner and macroscopically of worse quality. Increase of temperature was associated with higher secretion of hydrogen. The problem of gas bubbles was solved by fast stirring of the electrolytic bath, which also ensured the incorporation of TiO_2 particles in the Ni matrix. Coatings were deposited with the different current densities in the range 1 A/dm^2 - 2.5 A/dm^2.

Fig. 1 shows the SEM images of the microstructure of nc-TiO_2/Ni coatings deposited at different current densities. Obtained coatings were growing perpendicularly to the substrate, creating characteristic microstructure of electrodeposited nc-TiO_2/Ni composite deposited at the direct current [6]. Surface of coatings was rather rough, with cauliflower morphology,

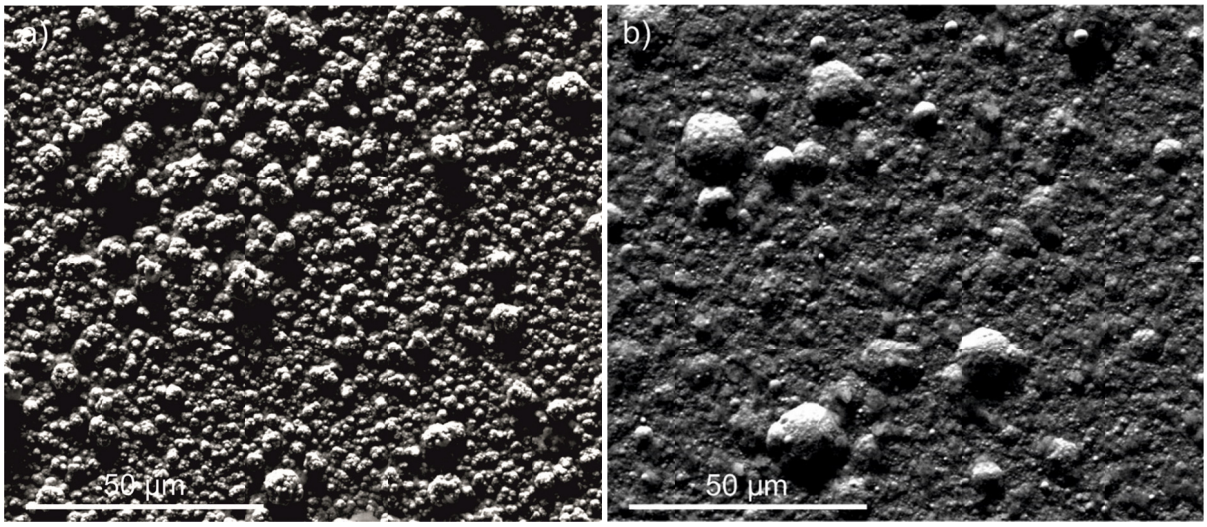

Fig. 1. Microstructure of nc-TiO_2/Ni coatings electrodeposited from baths containing 10 g/L of TiO_2 at current density equal a) 1 A/dm^2 b) 2.5 A/dm^2. SEM

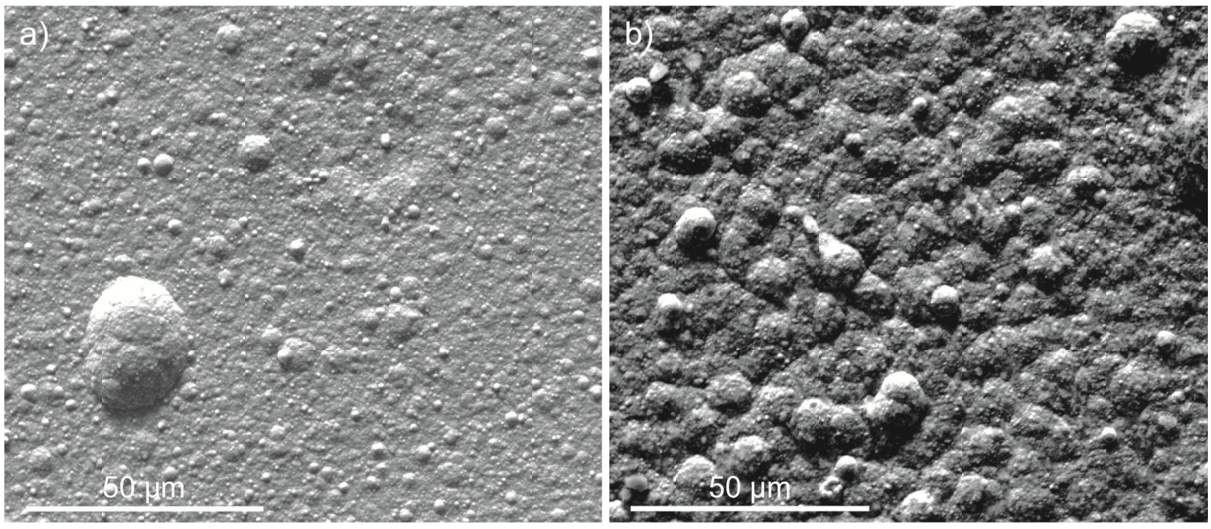

Fig. 2. Microstructure of nc-TiO_2/Ni coatings electrodeposited form baths containing a) 2g/L of TiO_2 b) 10g/L of TiO_2 at current density equal 2.5 A/dm^2. SEM

in which size and amount of nodules depended of deposition parameters. The size of nodules was influenced the inter alia by the current density. For the current density 1 A/dm^2 the diameter of nodules was about few micrometers and with increase of the current density for 2.5 A/dm^2 it enlarged over a dozen micrometres. The effect of the TiO_2 concentration on the morphology of the coating was also examined. It was observed that for the concentration of TiO_2 particles 2g/L the amount of the nodules was smaller than for the higher concentration of 10 g/L (Fig. 2).

Fig. 3 shows SEM image of the cross-section specimen of the coating. The undercoat Ni and Cu layers with thickness about 1 mm and the nc-TiO_2/Ni coating and thicker composite nc-TiO_2/Ni coating about 8 mm thick are marked. The layers are characterized by a good connection between them, without any discontinuities at the interfaces.

The TEM microstructural investigation revealed the nanocrystalline microstructure of nc-TiO_2/Ni coating (Fig. 4a). Selected area diffraction pattern (Fig. 4c) from the area marked

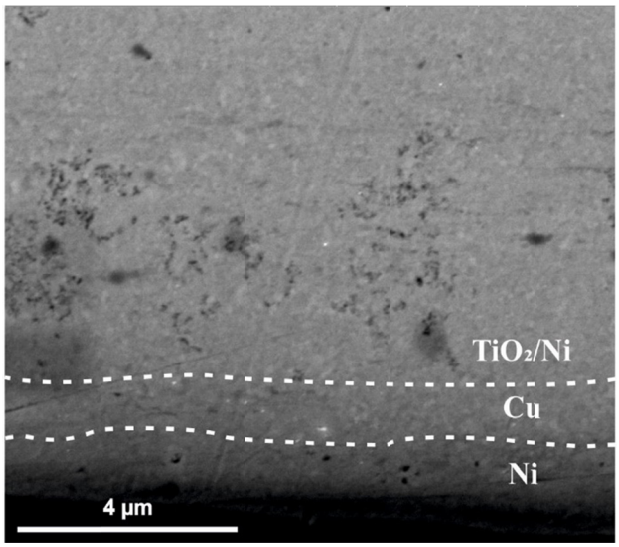

Fig. 3. Cross-section of nc-TiO_2/Ni coating electrodeposited form baths containing 10 g/L TiO_2. SEM

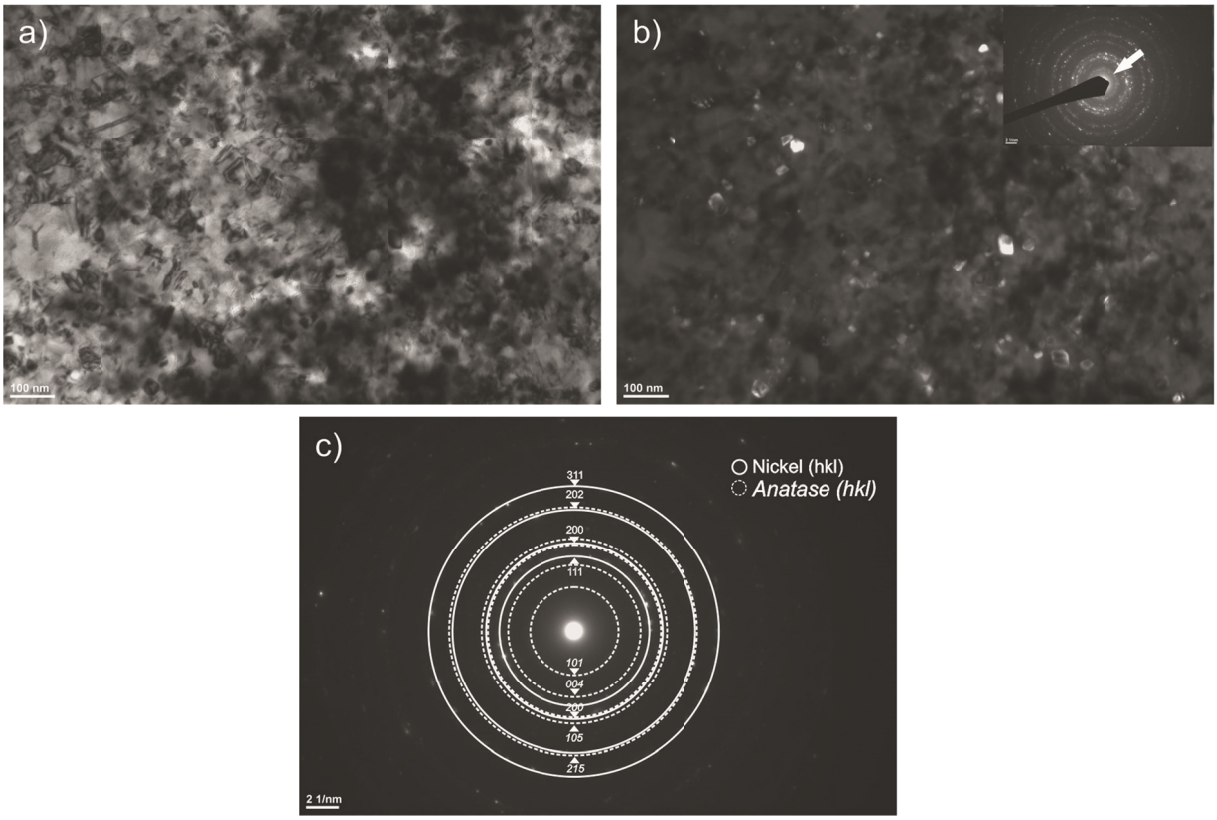

Fig. 4. a) TEM bright-field image, b) dark-field image of the TiO_2 particles in the (101) ring of anatase and c) selected area electron diffraction with its solution for nickel and anatase

by arrow in Fig. 4b contained rings from nickel and anatase. The dark-field image from anatase (101) ring (Fig. 4b) shows the homogeneous distribution of TiO_2 nanoparticles in the Ni matrix. The average diameter of nickel grains was 40±8.5 nm. The size of reinforcement grains was smaller and diameter of TiO_2 particles was in the range of 20 nm - 30 nm. Inside the Ni nanograins the twins were frequently observed (Fig. 5). It is in good agreement with the results obtained by Kumar et. al. [22], who have observed the formation of growth twins in electrodeposited nanocrystalline nickel films. The observation of the twinned microstructure suggests that the obtained composite can be strengthened both by the TiO_2 and the high density of planar defects.

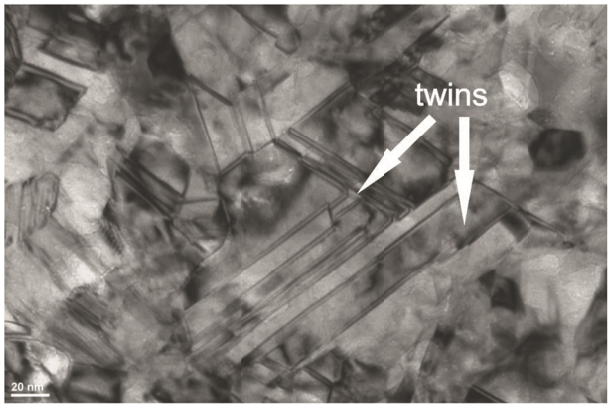

Fig. 5. TEM bright field image of nc-TiO_2/Ni coating showing growth twins inside Ni nanograins

STEM bright-field image of the coating microstructure and the corresponding Ni and Ti maps are given in Fig. 6. The Ti map reveals that TiO_2 particles are not evenly distributed at microscale and in some areas exhibit higher concentration. Possibility of more uniform dispersion of nanoparticles in the microstructure requires further studies on deposition conditions.

Corrosion resistance

Polarization curves acquired in Ringer's solution for uncoated 316L steel plate as well as coated with Ni and nc-TiO_2/Ni coating are present in Figure 7. Two important corrosion parameters, namely corrosion current density and corrosion potential were measured (Tab. 3). Based on the obtained results it can be concluded that both Ni and nc-TiO_2/Ni coatings improve corrosion resistance of the 316L steel in the Ringer's solution. Both coatings reduce the corrosion current density and corrosion potential compared to bare stainless steel. The corrosion current density of nc-TiO_2/Ni coatings was 0.317 $\mu A/cm^2$, what is about 10 times lower than for uncoated stainless steel. The corrosion potential for the composite coating was -0.122 V vs. Ag/AgCl electrode for the coating obtained for bath which contained 10 g/L TiO_2.

This parameter was significantly higher than for Ni coating (–0.275 V) and uncoated steel (–0.346 V). Addition of TiO_2 nanoparticles into Ni matrix moves potential into noble direction. The corrosion rate, which was measured from Tafel extrapola-

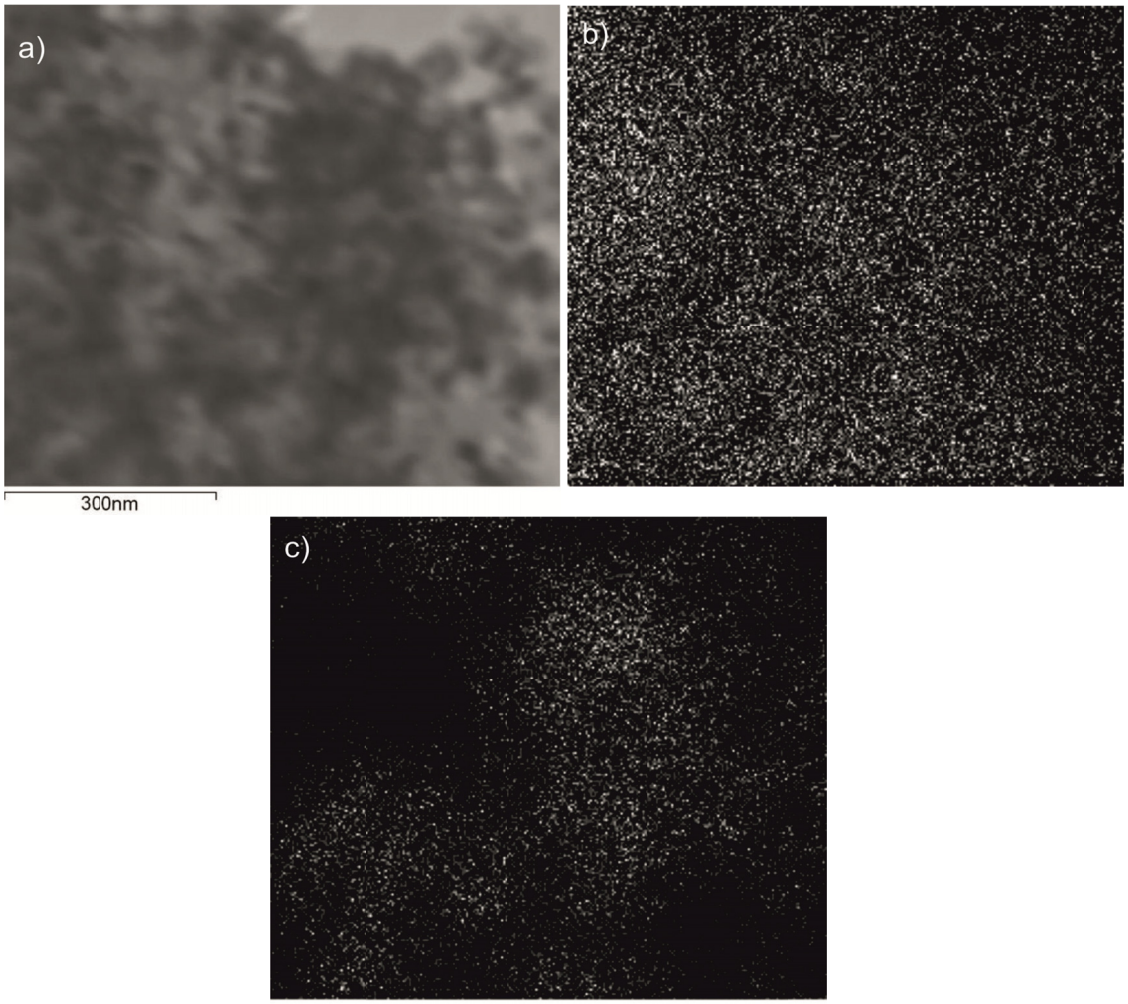

Fig. 6. a) STEM bright-field image as well as corresponding b) Ni and c) Ti EDS maps

tion, was 10 times lower for the composite coatings than for the bare steel and 4 times lower than for Ni coatings.

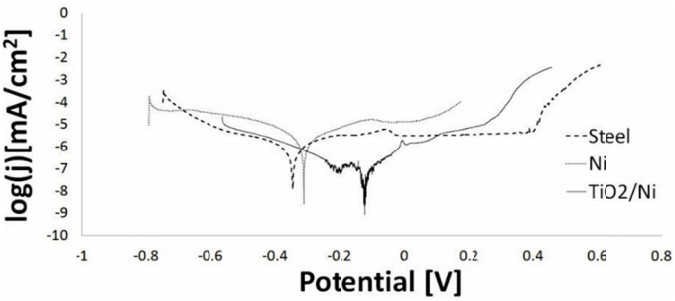

Fig. 7. Polarization curves for nc-TiO_2/Ni coatings and Ni on X2CrNiMo17-12-2 steel and for bare steel

Impedance spectroscopy analysis (EIS) was also applied to measure the resistivity of coatings, which depends on their porosity, adherence to the substrate and roughness. TiO_2 particles incorporated in the coating should increase the resistivity, decreasing the contact of corrosion media with substrate. The Nyquist plots and replacement circuit model are shown in Figs 8 and 9. The coatings before measurement were soaked in the Ringer's solution for 1 hour.

In all measurements the semicircles diameters from composite nc-TiO_2/Ni coatings were bigger than for pure Ni coatings. Simulated curves were well fitted for the simplest circuit, therefore it was not necessary to use more complicated model. The parameters of simulated circuit are shown in table 3. It was revealed that the results were in good agreement with those obtained by polarization curves measurements. The highest corrosion resistance was achieved for specimens with nc-TiO_2/Ni coatings. TiO_2 particles probably filled discontinuities in the coatings and reduced the interaction between corrosion media and steel substrate.

As it was reported in [5,15], the addition of TiO_2 to Ni matrix improves corrosion resistance, reduces corrosion cur-

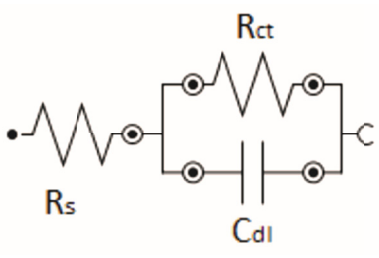

Fig. 8. Scheme of Randles equivalent circuit

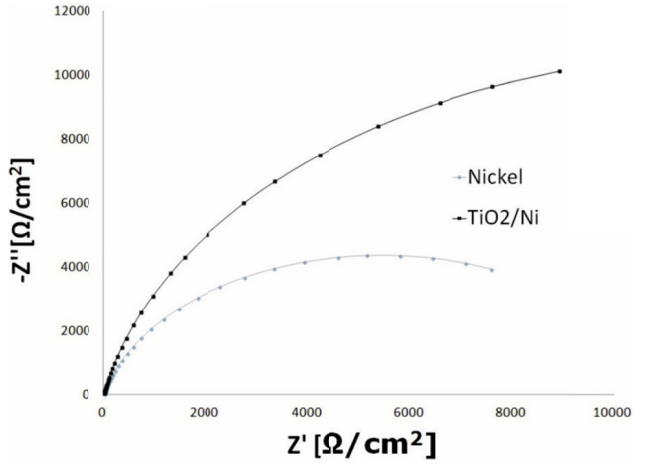

Fig. 9. Impedance spectra for Ni and nc-TiO_2/Ni coatings on X2CrNiMo17-12-2 steel

rent and increases resistivity of the coatings. The mechanism of improvement of corrosion resistance is common in ceramic/Ni composites obtained by electrodeposition and was confirmed for another ceramic materials like: Al_2O_3, SiC [23]. The increased corrosion resistance of the coating is connected with inert barrier created by TiO_2 particles in Ni matrix. Furthermore, the potential of TiO_2 is more positive that Ni matrix and it causes formation of corrosion cells, in which is TiO_2 acting as cathode and Ni as anode, what is beneficial for anodic protection of the coating [16].

TABLE 3

Selected parameters of corrosion resistance of Ni, nc-TiO_2/Ni coatings on steel and for bare steel

	E_{corr} [V]	i_{corr} [µA]	Corrosion wear [mm/year]	R_s [Ω]	R_{ct} [Ω]	C_{dl} [µF]
Steel 316L	–0,346	3,16	0,0368			
Ni	–0,275	1,28	0,0299	18,84	10866	64,2
10 g/L TiO_2/ Nikiel	–0,122	0,317	0,0049	17,34	25467	62,5

4. Conclusions

In this work the method of co-electrodeposition of nc-TiO_2/Ni coatings from citric-sulfate baths was applied. The influence of the nano-TiO_2 particles on the microstructure and electrochemical corrosion resistance was presented. Based on the results, it can be concluded that:

1. By the electrodepositon of nc-TiO_2/Ni is possible to obtain composite coatings with homogeneous distribution of nc-TiO_2 in Ni matrix.
2. The obtained composite nc-TiO_2/Ni coatings are characterized by nanocrystalline microstructure with high density of growth twins in Ni nanograins.
3. The nc-TiO_2/Ni coatings improve corrosion resistance of 316L steel in Ringer's solution. The corrosion rate of the steel coated by such nanocomposite coatings is smaller than in the case of nickel coatings.

Acknowledgment

The work was financially supported by the statutory project of AGH-UST no. 11.11.110.293.

The authors appreciate a valuable contribution in experiments of Mateusz Kopyściański, PhD from AGH-UST.

REFERENCES

[1] D. Thiemig, A. Bund, Surface and Coatings Technology **202**, 2976 (2008).
[2] S. Spanou, E.A. Pavlatou, N. Spyrellis, Electrochimica Acta **54**, 2547 (2009).
[3] S.A. Lajevardi, T. Shahrabi, Applied Surface Science **256**, 6775 (2010).
[4] G. Parida, D. Chaira, M. Chopkar, A. Basu, Surface & Coatings Technology **205**, 4871 (2011).
[5] G. Yılmaz, G. Hapc¸, G. Orhan, JMEPEG **24**, 709 (2015).
[6] L. Benea, E. Danaila, J.P. Celis, Materials Science&Engineering **A610**, 106 (2014).
[7] Tadashi Doi, Kazunari Mizumoto, Metal Finishing **102**, 104 (2004).
[8] L. Chaoqun, L. Xinhai, W. Zhixing, G. Huajun, Rare Metal Materials and Engineering **44** (7), 1561 (2015).
[9] D.H. Kim, S.Y. Kim, S.W. Han, Y.K. Cho, M.G. Jeong, E.J. Park, Y.D. Kim, Applied Catalysis A: General Volume **495**, 184 (2015).
[10] R. Zhou, N. Rui, Z. Fan, C. Liu, International Journal of Hydrogen Energy (2016).
[11] N.M. Mohamed, R. Bashiri, F.K. Chong, S. Sufian, S. Kakooei, International Journal of Hydrogen Energy **40**, 14031 (2015).
[12] H. Lin, C. Shih, Journal of Molecular Catalysis A: Chemical **411**, 128 (2016).
[13] A.J. Haider, A.A. Najim', M.A.H. Muhi, Optics Communications **370**, 263 (2016).
[14] S. Spanoua, A.I. Kontos, A. Siokouc, A.G. Kontos, N. Vaenas, P. Falaras, E.A. Pavlatoua, Electrochimica Acta **105**, 324 (2013).
[15] A. Katamipour, M. Farzam, I. Danaee, Surface & Coatings Technology **254**, 358 (2014).
[16] H. Goldasteh, S. Rastegari, Surface & Coatings Technology **259**, 393 (2014).
[17] Y. Wang, S.J. Wang, X. Shu, W. Gao, W. Lu, B. Yan, Journal of Alloys and Compounds **617**, 472 (2014).
[18] B. Ranjith, G. Paruthimal Kalaignan, Applied Surface Science **257**, 42 (2010).
[19] A. Laszczynska, J. Winiarski, B. Szczygieł, I. Szczygieł, Applied Surface Science **369**, 224 (2016).
[20] M.W. Khalil a , Taher A. Salah Eldin, H.B. Hassan , Kh. El-Sayed, Z. Abdel Hamid, Surface & Coatings Technology **276**, 89 (2015).
[21] L. Besra, M. Liu, Progress in Materials Science **52**, 1 (2007).
[22] K.S. Kumar, S. Suresh, M.F. Chisholm, J.A. Horton, P. Wang, Acta Materialia **51**, 387 (2003).
[23] S. Dehgahi, R. Amini, M. Alizadeh, Surface & Coatings Technology **304**, 502 (2016).